IMPEDANCE-BASED CONTROL OF THE MIT-SKYWALKER

Panagiotis K. Artemiadis
Newman Lab of Biomechanics
and Human Rehabilitation
Department of Mechanical Engineering
Massachusetts Institute of Technology
Cambridge, MA 02139
Email: partem@mit.edu

Hermano Igo Krebs
Newman Lab of Biomechanics
and Human Rehabilitation
Department of Mechanical Engineering
Massachusetts Institute of Technology
Cambridge, MA 02139
Email: hikrebs@mit.edu

ABSTRACT

Walking impairments are a common sequela of neurological injury, severely affecting the quality of life of both adults and children. Gait therapy is the traditional approach to ameliorate the problem by re-training the nervous system and there have been some attempts to mechanize such approach. In this paper, we present a novel impedance controller for the MIT-Skywalker. In contrast to previous approaches in mechanized gait therapy, the MIT-Skywalker does not impose a rigid kinematics pattern of normal gait on impaired walkers. Instead, it takes advantage of the concept of passive walkers and the natural dynamics of the lower extremity in order to deliver more "ecological" therapy. The proposed closed-loop control scheme can regulate the interaction between the walker and the treadmill and can provide the appropriate feedback to the walker during stance phase as well as at heel-strike and toe-off. Simulation results prove the feasibility of the impedance-based control scheme.

INTRODUCTION

Every 40 seconds, someone in the United States has a stroke [1]. For every 1,000 children born in the US, 2.8 youngsters have cerebral palsy [2]. The impact of these and other neurological pathologies–such as spinal cord injury, multiple sclerosis, Parkinson–on walking is significant and locomotor capacity is a critical factor in determining an individual's degree of disability and potential for falling. Physical and occupational therapy are the standard of care to educate the individual on how to compensate for his/her impairment and how to ameliorate or regain walking abilities. Recovery is a slow process with significant demands on the therapist. We introduced a paradigm shift in 1989 when we started the development of the MIT-Manus [3]. The goal was to provide robotic tools to facilitate and increase the productivity of clinicians while optimizing the potential for patients to recover.

Regarding gait therapy, the most common mechanical device used is the treadmill since it offers repetitive movements that can improve muscular strength, aerobic capacity, and movement coordination [4]. In most cases, the treadmill is used in conjunction with a body weight support that has been shown to improve gait and lower-limb motor function in patients with gait disorders [5], [6]. Such repetitive practice in task-oriented fashion has been proved to lessen disability of lower limbs and improve walking. More specifically, body weight-supported treadmill training (BWSTT) for hemiparetic stroke patients has been shown to improve balance, lower-limb motor recovery, walking speed, endurance, and other important gait characteristics such as symmetry and stride length [7].

However, BWSTT requires a therapist to monitor and manipulate the pelvis in addition to one or two therapists needed to propel the leg(s) forward. Robotic devices were built in an attempt to automate the therapy process further. While several robotic devices already exist (e.g., MIT's Anklebot [8], KineAssist [9], Haptic Walker, G-EO, UC Irvine's Pam and Pogo [10], Lopes [11], Motorika/Healthsouth Autoambulator), presently only two devices have been used extensively with more than 20 patients with published outcomes, namely the Gait Trainer I and the Lokomat. Gait Trainer I is an end-effector based robot with quick set-up time, incorporating both an adjustable Body Weight Support (BWS) and sliding foot plates that are secured to the patient's feet [12]. While it minimizes the number of therapists to only one needed to manipulate the knee, the planar

sliding motion reproduces the kinematic of gait but it does not reproduce heel-strike. The Gait Trainer I was tested in a large multi-site RCT, DEGAS study, with positive results [12]. The Lokomat system is an exoskeletal device. It includes a treadmill, adjustable and active BWS (newest generation) designed to provide a constant level of support throughout the gait cycle, and a robotic orthosis with four degrees of freedom, actuating left and right knee and hip joints [13]. This device attempts to replicate the kinematics of an unimpaired subject. It does not incorporate any means to promote weight shifting from one leg to the other, hence requiring the use of the body-weight system to unload the legs and facilitate propulsion of the leg forward. It also forces the ankle to be always in a dorsiflexed position. Although there were some positive pilot results using the Lokomat [14], more recent studies found that Lokomat training had no advantage compared to conventional therapy [15], [7]. Because of the much higher intensity of training in the Lokomat group, we interpreted this result as an indication that the Lokomat kinematic experience might not be affording the proper neurological stimulus.

Previous studies have shown that the spinal locomotor pools, which include a central pattern generator for activity of automatic, alternating flexor, and extensor leg muscles, are highly responsive to phasic segmental sensory inputs and show evidence of learning during step training [16]. Therefore, providing the appropriate sensory input to the patient is very critical. More specifically, at the transition between the stance and swing phase, i.e., the heel-strike and the toe-off, the appropriate stimulation from the environment is shown to be critical. However, most of the previous robotic devices used for gait therapy do not distinguish those events, imposing rigid or non-controlled interaction of the patient's foot with the treadmill. In this way, the required sensory input is not provided to the user, and the benefit of central pattern generators being responsive to those inputs is not exploited.

We have recently introduced to the clinic the MIT-Skywalker [17]. This novel rehabilitation robot is unique and distinct from any other existing rehabilitation robotic devices for gait. It delivers safe and efficacious gait therapy inspired by the concept of passive walkers [18]. Contrary to the kinematic-based gait robots, the MIT-Skywalker creates the required ground clearance for swing while exploiting gravity to assist during leg propulsion. Preliminary tests with a mannequin and unimpaired subjects, using a camera-based closed loop control architecture, demonstrated the MIT-Skywalker's ability to allow gait therapy without restricting the movement to a rigid kinematic profile, thereby providing ecological heel-strike and hip-extension and maximizing patient participation during therapy. Moreover, since the working principle is based on the dynamics of the leg, it doesn't require any mechanism attached on the patient's leg, maximizing safety and minimizing significantly the time for don-on and -off.

In this paper, an impedance-based controller is introduced in order to regulate the patient's leg and treadmill interaction during heel-strike, toe-off, as well as the duration of the stance phase.

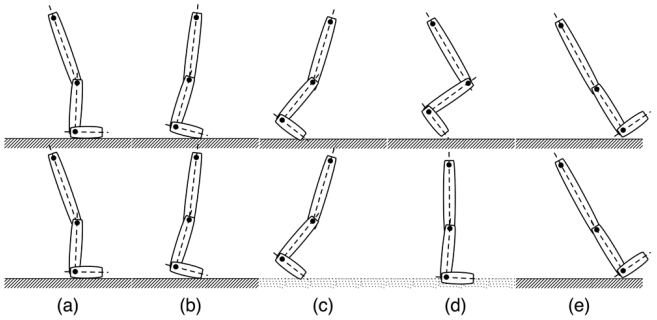

Figure 1. Gait phases for walking on a flat surface (top row) and a surface that drops between toe-off (c) and heel strike (e) (bottom row).

Controlling the impact of the leg with the treadmill during heel-strike provides the patient with the appropriate sensory feedback, while it prevents high-torque development at leg joints and inappropriate leg configuration that can result in patient injury. Moreover, the leg trajectory imposed by the treadmill during the stance phase and at toe-off is controlled with an impedance controller, which regulates the interaction between the leg and the treadmill at the vertical axis of treadmill motion. Simulation results demonstrated the feasibility of the impedance-based control scheme, and we should initiate pilot clinical trials shortly

DESCRIPTION OF THE MIT-SKYWALKER

In conventional gait physiotherapy, the therapist pushes or slides the patient's swing leg forward, either on the ground or on a treadmill. In the kinematically-based robot-assisted gait therapy, the leg is propelled by either the robot orthosis acting on the patient's leg (in Lokomat), or foot plates attached on the patient's foot (in Gait Trainer I). Instead of lifting the patient's leg manually or mechanically, we achieve forward propulsion in the MIT-Skywalker by lowering the walking surface. This provides both swing clearance and takes advantage of dynamics and gravity to propel the leg forward while allowing proper neural inputs for hip extension and ecological heel strike. Figure 1 illustrates those phases.

It must be noted that the replication of the exact gait kinematics is not required in the MIT-Skywalker. For example, during the swing phase the leg behaves as a free double pendulum, not accommodating significant knee flexion, as in normal gait. However, it has been shown in previous studies with stroke patients using the Lokomat system [14], that the replication of natural gait kinematics is not effective [15], [7]. The MIT-Skywalker will allow for evidence-based therapy engaging the dynamics of the leg without imposing rigid kinematics patterns of normal gait.

Our alpha-prototype was built in order to accommodate foot clearance for patients in the range of the 99th percentile adult male and the 1st percentile adult female. It includes a body-weight support system, since many patients are not able to support their weight on the impaired leg(s) or they may need assistance maintaining balance. This system provides enough support to unload up to 100% of the patient's weight and keep the pa-

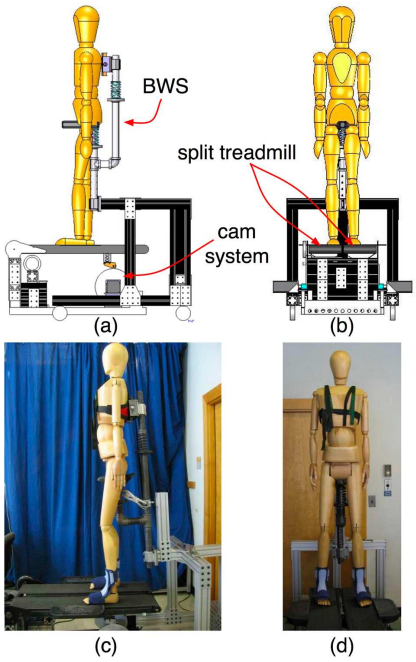

Figure 2. The MIT-Skywalker. (a), (b): Side and front views of the model, where the Body-Weight Support (BWS), the two treadmills and the cam system are shown. (c), (d): Side and front views of the actual platform built with a human-sized mannequin sitting on it.

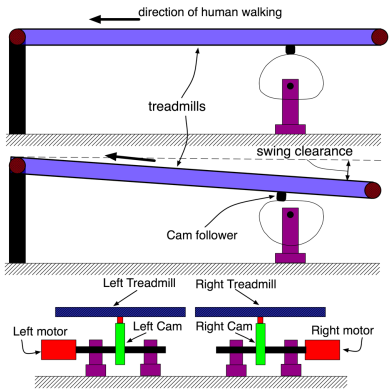

Figure 3. Side and front views of the cam systems actuating the two treadmills.

Table 1. Cam Profile Specifications

Maximum motor speed (rad/sec)	40
Swing duration (sec)	0.8
Treadmill clearance (m)	0.09
Minimum cam radius (m)	0.063

tient safe from falls, yet not interfere with the required ranges of leg motion. While kinematically-based devices employ overhead full-body harnesses, we designed a system to afford fast don-on and -off. It consists of a simple chest harness providing stabilization for the upper body and a saddle-like seat for body-weight support. More details on the hardware architecture and characteristics of the MIT-Skywalker can be found elsewhere [17]. Moreover, the MIT-Skywalker must provide a stable walking surface that is parallel to the ground, allow adequate clearance for the patient's leg to swing without knee flexion, and return to the horizontal plane in time for the heel strike of the next stride, as shown in Fig. 1. The walking surface for each leg is a treadmill, which stays horizontal during the stance phase and may be lowered to provide swing clearance to the impaired leg. The alpha-prototype includes a split treadmill system and a cam to lower the tracks as shown in Fig. 2. The cam system for lowering each treadmill is depicted in Fig. 3. Finally, the cam is actuated by a brushless motor coupled with a gearbox (gear ratio 20:1). The motor is controlled in real-time in torque. The velocity of the motor actuating the treadmill is also controlled in real-time.

The cam profile characteristics were appropriately defined so that the treadmill was lowered enough to provide the required clearance for the swing of the leg. Moreover, the treadmill should be raised on time for the heel-strike to occur. Therefore, given the maximum speed of the motor used for actuating the cam and the duration of the swing phase for walking speeds usually found in gait therapy (1 - 1.5 miles per hour), the profile specifications of the cam were defined. In order to provide smooth treadmill acceleration during lowering and rising, a 3rd order polynomial was used to define the cam profile in polar coordinates. The final cam profile for the treadmill actuation is shown in Fig. 4a, while Table 1 lists the specifications taken into consideration for the design of the cam profile. The computed profile of the cam was replicated three times, as shown in Fig. 4b, to allow for future applications with greater walking speeds.

The control of the cam system is key in providing the required swing clearance for the patient's leg and ecological hip-extension and heel-strike. Although we can probe the state of the device, we required feedback of the patient's leg so as to control the treadmill speed and cam system. For this reason, we experimented with a simple camera-based motion tracking technique. It provides both flexibility and safety for the patient, requiring no sensors mounted on the patient's leg except for a small, easy-to-place marker. The marker is red-colored and has the shape of a circle with an approximate radius of 20mm, and is placed on the heel side (sides of the calcaneus bone) of each leg. Low-cost cameras (Logitech Webcam Pro 900, Logitech Inc.) are placed at each side of the device. The range of motion of the heel in the sagittal plane during normal walking (approx. 130 cm in the horizontal axis and 50 cm in the vertical axis [19]), along with the angle of view of the camera (approx. 60°), resulted in a camera positioning distance from the tracked marker of 110 cm. The camera is providing high-resolution, colored images at the frequency of 30 Hz, which is adequate for the timing requirements of the control of the treadmill vertical motion during normal walking. The setup with the cameras and the markers is depicted in Fig. 5, while details on the camera-based controller can be found in [20]. Finally, it must be noted that the present system with the cam requires almost 0.5m from the floor to afford the necessary clearance to lower the treadmill. We are

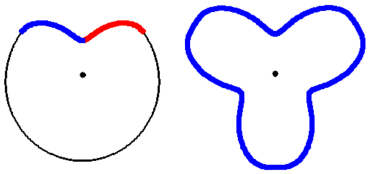

Figure 4. (a) Two 3^{rd} order polynomials (blue and red), in polar coordinates, were used for defining smooth cam profile with the required clearance. (b) The resulted cam profile after replicating the polynomial three times around the cam.

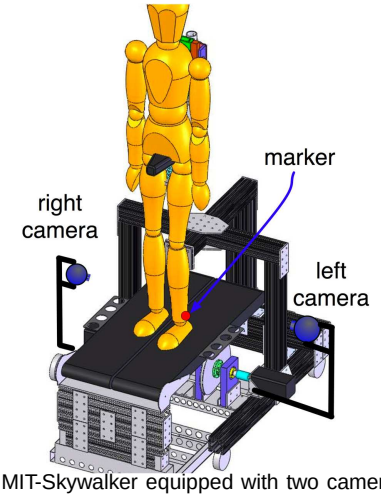

Figure 5. The MIT-Skywalker equipped with two cameras on the sides to monitor the position of the red markers placed on the user's heels.

investigating alternative approaches to reduce this height.

Impedance-Based Control Architecture

An impedance-based control architecture was developed for the monitoring and control of the interaction between the leg and the treadmill. This consisted of two main parts: the planner and the impedance controller. The planner essentially defines the impedance characteristics of the cam-actuated treadmill based on the position of the leg of the patient during the gait cycle. Having the desired impedance characteristics defined, a controller was designed for actuating the cam in order to exert the desired forces at the leg.

Planning Algorithm: The planning algorithm was used to define the impedance characteristics of the treadmill, based on the phase of the gait the leg is at. Therefore, three distinct phases/events were defined:

(1) The heel-strike: it occurs at the end of the swing phase, as soon as the heel of the leg reaches the treadmill horizontal level. At the heel-strike, the desired impedance of the treadmill is characterized as high. This is to provide the appropriate feedback to the patient that the foot has landed. The virtual (desired) position of the heel is defined at the horizontal axis of the treadmill, at a point that is computed online, based on the achieved stride length of the leg. In other words, as soon as the heel is ready to land on the treadmill, the virtual point is placed at the projection of the pre-landing heel position at the treadmill level. Let P_h be the virtual point at heel-strike, with coordinates $\begin{bmatrix} x_h & y_h \end{bmatrix}^T$.

(2) The stance phase: it lasts from the heel-strike to the toe-off phase, during which the leg travels to the back end of the treadmill preparing for the toe-off phase. During the stance phase, the virtual (desired) trajectory is generated using the heel-strike position and the desired toe-off position as initial and final points respectively. The trajectory at the x axis is generated by a linear equation given by:

$$x_s(t) = x_h + \gamma t \tag{1}$$

where $x_s(t)$ is the trajectory component in the x axis as a function of time t, and γ is a velocity component that defines the desired leg velocity along the x axis given by:

$$\gamma = \frac{s}{t_f} \tag{2}$$

where $|s|$ is the desired stride length, $s < 0$, and t_f the desired time for this stride, where $t = 0$ at heel-strike. The trajectory at y axis is generated by a 4^{th} order polynomial equation given by:

$$y_s(t) = a_0 + a_1 t + a_2 t^2 + a_3 t^3 + a_4 t^4 \tag{3}$$

where $y_s(t)$ is the trajectory component in the y axis as a function of time t, while the parameters a_0, a_1, a_2, a_3, a_4 are computed using the following boundary conditions:

$$\begin{aligned} &y_s(0) = y_h \qquad && y_s(t_f) = y_t \\ &y_s\left(\tfrac{t_f}{2}\right) = y_{s_0} && \dot{y}_s(0) = 0 \\ &\dot{y}_s(t_f) = 0 \end{aligned} \tag{4}$$

where y_t is the coordinate of the toe-off point at the y axis, and y_{s_0} is the lowest coordinate of the heel at mid-stance. The choice of the order of polynomial was done based on the available number of boundary conditions 4. Note that a non-zero value for $\dot{y}_s(0)$ and $\dot{y}_s(t_f)$ could be selected to augment the sensory information during landing and we will investigate such modifications during clinical testing. Values for the duration of stance phase are estimated using the current walking speed and approximations for normal gait patterns based on the literature [19]. Moreover, the lowest point during mid-stance is based on measurements of typical pelvis vertical motion during ground walking reported in the literature [21]. Since pelvic motion is not fully accommodated

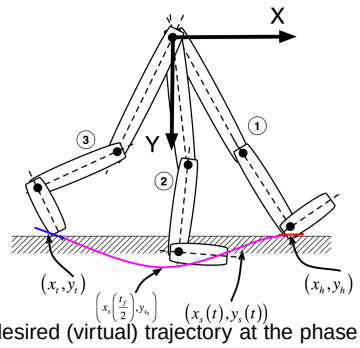

Figure 6. The desired (virtual) trajectory at the phase of heel-strike (1), the stance phase (2) and toe-off (3).

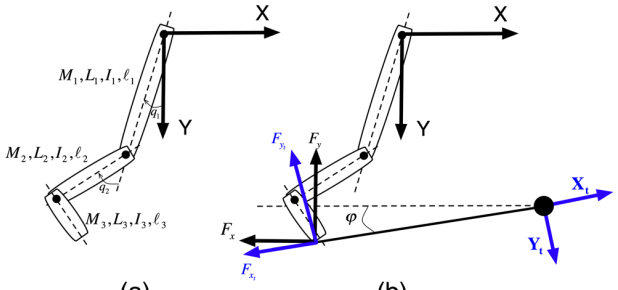

Figure 7. (a) The leg is modeled as a 2 degrees-of-freedom mechanism. Each limb segment (thigh, shank, foot) have individual dynamic parameters: mass (M_i), total length (L_i), inertia with respect to center of mass (I_i), distance from joint to center of mass (ℓ_i), $i = 1,2,3$. (b) Forces exerted at the contact point of the treadmill with the leg, with respect to the global (black) and treadmill reference system (blue).

by the MIT-Skywalker, the desired leg profile is constructed by mirroring the pelvis motion at the level of the treadmill. In other words, the pelvis motion during normal gait, which is not accommodated by the MIT-Skywalker, is transferred to the treadmill in order to mimic as much as possible natural gait kinematics. Finally the parameters a_0, a_1, a_2, a_3, a_4 are given by:

$$\begin{aligned} a_0 &= y_h \\ a_1 &= 0 \\ a_2 &= \frac{-11y_h + 16y_{s_0} - 5y_t}{t_f^2} \\ a_3 &= \frac{18y_h - 32y_{s_0} + 14y_t}{t_f^3} \\ a_4 &= -\frac{8y_h - 16y_{s_0} + 8y_t}{t_f^4} \end{aligned} \tag{5}$$

(3) The toe-off: it occurs after the heel has left the treadmill level and the leg is ready to swing forward. The heel is at the far most point at the horizontal axis. Let P_t be the virtual point at toe-off, with coordinates $\begin{bmatrix} x_t & y_t \end{bmatrix}^T$, which are defined in order to provide the required initial conditions for the free leg swing phase.

The phases/events along with the desired virtual trajectories are shown in Fig. 6.

Impedance Controller: An impedance controller was designed to command the vertical motion of the treadmill. Only the motion of the leg at the sagittal plane is considered. The ankle joint is considered fixed and at neural position. This is a practice that was also followed in the experiments with unimpaired subjects, in order to simulate the prevention of drop-foot and allow the treadmill to provide the necessary swing clearance [20]. Lastly, it is assumed in our design that the leg is completely passive, i.e., there is no voluntarily actuated torque at the leg joints.

The leg is modeled as a 2 degrees-of-freedom mechanism, as shown in Fig. 7a. Leg dynamics are described by the following equation

$$\mathbf{M}(\mathbf{q})\ddot{\mathbf{q}} + \mathbf{C}(\mathbf{q},\dot{\mathbf{q}})\dot{\mathbf{q}} + \mathbf{G}(\mathbf{q}) = \mathbf{0} \tag{6}$$

where $\mathbf{q} = \begin{bmatrix} q_1 & q_2 \end{bmatrix}^T$, $\dot{\mathbf{q}}$, $\ddot{\mathbf{q}}$ are the angular position, velocity and acceleration vectors, q_1, q_2 the hip and knee joint angles respectively as shown in Fig. 7a, $\mathbf{M}(\mathbf{q})$, $\mathbf{C}(\mathbf{q},\dot{\mathbf{q}})$ are the inertia and Coriolis-centrifugal matrices, and $\mathbf{G}(\mathbf{q})$ the gravity vector. The leg is assumed completely passive; therefore no actuating torques are included. In addition, friction and stiffness phenomena are omitted for simplicity.

When the leg is in contact with the treadmill, the latter is exerting force to the leg at the contact point. Let $\mathbf{F}_f = \begin{bmatrix} F_{x_f} & F_{y_f} \end{bmatrix}^T$ be the force exerted to the leg contact point when the treadmill is in horizontal position. In the general case where the treadmill is inclined with respect to the horizontal axis for an angle φ (see Fig. 7b), the force exerted to the leg is given by:

$$\mathbf{F}_f = \begin{bmatrix} \cos(\varphi) & -\sin(\varphi) \\ \sin(\varphi) & \cos(\varphi) \end{bmatrix} \mathbf{F}_t \tag{7}$$

where $\mathbf{F}_t = \begin{bmatrix} F_{x_t} & F_{y_t} \end{bmatrix}^T$ is the force exerted by the treadmill, defined with respect to the treadmill reference system $\langle X_t, Y_t \rangle$.

Eq. (6), including the treadmill-exerted force, can be rewritten in Cartesian space as follows:

$$\mathbf{M}_x(\mathbf{q})\ddot{\mathbf{x}} + \mathbf{C}_x(\mathbf{q},\dot{\mathbf{q}}) + \mathbf{G}_x(\mathbf{q}) = \mathbf{F}_f \tag{8}$$

where $\mathbf{x}$ is the position of the leg-treadmill contact point at the Cartesian space, and

$$\begin{aligned} \mathbf{M}_x(\mathbf{q}) &= \mathbf{J}(\mathbf{q})^{-T}\mathbf{M}(\mathbf{q})\mathbf{J}(\mathbf{q})^{-1} \\ \mathbf{C}_x &= \mathbf{J}(\mathbf{q})^{-T}\left(\mathbf{C}(\mathbf{q},\dot{\mathbf{q}}) - \mathbf{M}(\mathbf{q})\mathbf{J}^{-1}\dot{\mathbf{J}}\right)\dot{\mathbf{q}} \\ \mathbf{G}_x &= \mathbf{J}(\mathbf{q})^{-T}\mathbf{G}(\mathbf{q}) \end{aligned} \tag{9}$$

where $\mathbf{J}(\mathbf{q})$ is the Jacobian matrix relating joint and Cartesian coordinates. It must be noted that since the contact point between

the leg and the treadmill varies during the leg-treadmill interaction, two distinct cases were considered for simplicity. During heel-strike and the stance phase, the contact point is considered as being the heel, while at the last part of the stance phase and at toe-off, the toes are considered as the contact point.

Let $\mathbf{x}_0 = \begin{bmatrix} x_0 \; y_0 \end{bmatrix}^T$ be the virtual (i.e. desired) point at the Cartesian space, as it was defined by the planning algorithm analyzed above, i.e.

$$\mathbf{x}_0 = \begin{cases} \begin{bmatrix} x_h \; y_h \end{bmatrix}^T, & \text{at heel} - \text{strike} \\ \begin{bmatrix} x_s(t) \; y_s(t) \end{bmatrix}^T, & \text{during stance phase} \\ \begin{bmatrix} x_t \; y_t \end{bmatrix}^T, & \text{at toe} - \text{off} \end{cases} \tag{10}$$

while the continuity and smoothness of the switching planning scheme were guaranteed through the boundary conditions defined in 4. Then, the proposed control law is given by:

$$\mathbf{u}_f = \mathbf{M}_x(\mathbf{q})(\ddot{\mathbf{x}}_0 + \mathbf{B}_x\dot{\mathbf{e}}_x + \mathbf{K}_x\mathbf{e}_x) + \mathbf{C}_x(\mathbf{q},\dot{\mathbf{q}}) + \mathbf{G}_x(\mathbf{q}) \tag{11}$$

where

$$\mathbf{e}_x = \mathbf{x}_0 - \mathbf{x} \tag{12}$$

is the error between the virtual (desired) and the actual contact point position. It must be noted that the introduction of $\ddot{\mathbf{x}}_0$ in 11 is used to compensate for the leg's inertia dynamics. With the proper selection of the profile of $\ddot{\mathbf{x}}_0$, the closed-loop system behaves as a second-order system, whose behavior is controlled and bounded from the proposed controller in 11. The application of this controller results to the closed-loop dynamic equation, i.e.

$$\ddot{\mathbf{e}}_x + \mathbf{B}_x\dot{\mathbf{e}}_x + \mathbf{K}_x\mathbf{e}_x = \mathbf{0} \tag{13}$$

Therefore, by the proper selection of the gain matrices $\mathbf{B}_x$, $\mathbf{K}_x$, which essentially define the poles of the closed-loop system, the latter's stability is guaranteed. What is more, these gain matrices essentially describe the overall treadmill impedance. Finally it must be noted that since the subject's leg is modeled as a two-link two-degrees-of-freedom mechanism, both joint angles (i.e., hip and knee flexion-extension) are controllable using the proposed controller.

The remaining issue then is how to control the treadmill in order to exert the desired forces computed by the proposed control law, given by:

$$\begin{bmatrix} F_{x_t} \\ F_{y_t} \end{bmatrix} = \begin{bmatrix} \cos(\varphi) & \sin(\varphi) \\ -\sin(\varphi) & \cos(\varphi) \end{bmatrix} \mathbf{u_f} \tag{14}$$

Based on the assumption that the friction forces at the treadmill tape and the gravitational forces exerted from the leg to the treadmill are both constant and that there is no slippage of the leg

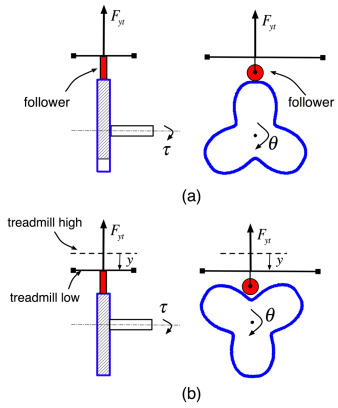

Figure 8. (a) Front and side view of the cam actuating the treadmill. The treadmill is at the horizontal (high) position. (b) Front and side view of the cam when the treadmill is lowered.

when it is in contact with the treadmill, the horizontal force F_{x_t} at the treadmill reference system is directly controlled by the treadmill velocity. Consequently, if ω_1 is the velocity of the motor actuating the treadmill and it can be controlled from the voltage commanded to this motor, then the horizontal force at the treadmill reference system is given by:

$$F_{x_t} = k\omega_1 \tag{15}$$

where k is a constant representing combined mechanical and geometrical factors involved in relating the motor speed and the applied force. This constant can be estimated using the motor specifications, geometric characteristics of the transmission mechanisms and estimation of friction forces at the treadmill belt. The vertical force F_{y_t} at the treadmill reference system is given by the following equation, assuming no friction at the follower (see Fig. 8):

$$F_{y_t} = \frac{\tau\omega_2}{\dot{y}} \tag{16}$$

where ω_2 is the rotational velocity of the cam, τ is the applied torque at the cam, and y the follower vertical displacement due to the cam profile, where $y = 0$ when the treadmill is at horizontal position. Let θ be the angular position of the cam with respect to its axis of rotation, and $\dot{\theta} = \omega_2$. Let

$$y = f(\theta) \tag{17}$$

where f is a continuous differentiable function that relates the vertical displacement of the follower with the angular position of the cam. This function can be easily computed from the cam profile design, since it describes the cam profile in polar coordinates. Details of the derivation of the function f are out of the scope of this paper. Then from (16), (17) we can compute the

torque to be commanded at the motor actuating the cam, given the desired vertical force F_{y_t}, by the following equation:

$$\tau = F_{y_t} \frac{df(\theta)}{d\theta} \tag{18}$$

Lastly, the desired impedance characteristics of the treadmill at each phase/event can be controlled through the assigned values for the matrices $\mathbf{B}_x$, $\mathbf{K}_x$ in (11). This is done again distinctively for each case, as shown below.

$$\mathbf{B}_x = \begin{cases} \mathbf{B}_{x_h}, & \text{at heel} - \text{strike} \\ \mathbf{B}_{x_s}, & \text{during stance phase} \\ \mathbf{B}_{x_t}, & \text{at toe} - \text{off} \end{cases}$$
$$\mathbf{K}_x = \begin{cases} \mathbf{K}_{x_h}, & \text{at heel} - \text{strike} \\ \mathbf{K}_{x_s}, & \text{during stance phase} \\ \mathbf{K}_{x_t}, & \text{at toe} - \text{off} \end{cases} \tag{19}$$

where $\mathbf{B}_{x_h} > \mathbf{B}_{x_s} > \mathbf{B}_{x_t}$, and $\mathbf{K}_{x_h} > \mathbf{K}_{x_s} > \mathbf{K}_{x_t}$. We selected a larger impedance value during the impact of the leg to the treadmill than during the stance and toe-off phase because the heel-strike sensory feedback might be an important cue for retraining gait. During stance phase, the impedance should be smaller to allow the treadmill to comply with possible deviations from the desired trajectory. At toe-off, the treadmill should be primarily elastic, in order to help the leg to acquire the necessary initial conditions for the initiation of the swing phase.

SIMULATION RESULTS

The controller was tested in simulation using the parameters listed in Table 2. The desired (virtual) trajectory was simulated by a 4^{th} order polynomial. The results of the leg tracking the trajectory are shown in Fig. 9a. The diagonal values of the gain matrices used are listed in Table 2. It must be noted that the same gains were used for both axes; therefore only one value is reported in Table 2.

In order to test the robustness of the method, we simulated muscle activation at the leg by input disturbance torque at both hip and knee joints. These can be assumed to be some of the responses generated by the patient in cases where the leg is not completely passive. The results of the leg tracking in the case where a torque disturbance is active for three short periods during stance are shown in Fig. 9b. The impedance characteristics were the same as in the previous case where the leg was considered completely passive. Differences in deviations from the virtual (desired) trajectory in those three instances are due to different forces exerted from the subject's leg to the treadmill in Cartesian space, since input disturbance was introduced in joint space, and the leg configuration differs among the three instances. These torque disturbances can also simulate inaccurate assumptions for leg dynamics for which parameter values are needed for the proposed controller as defined in (11).

Table 2. Simulation Parameters

Leg Dynamics					
$M_1\ (Kg)$	8.00	$M_2\ (Kg)$	3.72	$M_3\ (Kg)$	1.16
$L_1\ (m)$	0.47	$L_2\ (m)$	0.45	$L_3\ (m)$	0.27
$I_1\ (Kgm^2)$	0.32	$I_2\ (Kgm^2)$	0.14	$I_3\ (Kgm^2)$	0.06
$\ell_1\ (m)$	0.20	$\ell_2\ (m)$	0.19	$\ell_3\ (m)$	0.11
Impedance Values					
$B_{x_h}\ (\frac{Ns}{m})$	4.50	$B_{x_s}\ (\frac{Ns}{m})$	3.50	$B_{x_t}\ (\frac{Ns}{m})$	2.00
$K_{x_h}\ (\frac{N}{m})$	6.00	$K_{x_s}\ (\frac{N}{m})$	4.50	$K_{x_t}\ (\frac{N}{m})$	2.50
Virtual Trajectory Parameters					
$x_h\ (m)$	0.50	$y_h\ (m)$	0.90	$\gamma\ (\frac{m}{\text{sec}})$	1.25
$y_{s_0}\ (m)$	0.95	$y_t\ (m)$	0.80	$t_f\ (s)$	0.80

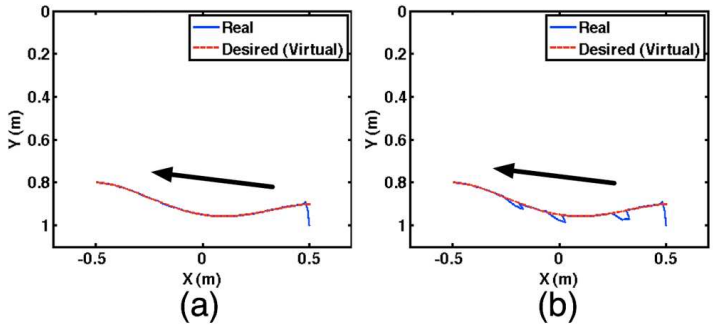

Figure 9. The desired and real trajectory of the leg end-point with the proposed controller with no external disturbances (a), and with simulating three torque disturbances in the leg joints during the stance phase (b). The arrow shows the direction of motion. The leg is initially positioned lower than the desired point at heel-strike.

CONCLUSIONS AND DISCUSSION

As robot-assisted gait therapy is increasingly gaining acceptance at rehabilitation centers, the MIT-Skywalker may prove to be the most effective and low-cost gait rehabilitation device. The fast don and doff alongside its dynamic principle and ecological intervention may place this novel device apart from the existing kinematically-based rehabilitation devices. As a final point, the proposed impedance-based control scheme may prove very efficient in delivering the desired sensory input to the patient, which would aid in his/her regaining lower limb control and walking ability.

We will be deploying the MIT-Skywalker to the clinic shortly and it will include many other features for promoting active participation of the patient.

ACKNOWLEDGMENT

Dr. H. I. Krebs and C. J. Bosecker have filed for patent protection. Dr. Krebs holds equity positions in Interactive Motion Technologies, Inc., the company that manufactures this type of technology under license to MIT. Dr. Panagiotis Artemiadis is being supported by a grant from the Cerebral Palsy International Research Foundation (CPIRF) and the Niarchos Foundation.

REFERENCES

[1] Heart disease and stroke statistics 2009 update: A report from the american heart association statistics committee and stroke statistics subcommittee [online].

[2] Jorgensen, H., Nakayama, H., Raaschou, H., Vive-Larsen, J., Stoier, M., and Olsen, T., 1995. "Outcome and time course of recovery in stroke. part i: Outcome. the Copenhagen stroke study.". *Arch.Phys.Med.Rehabil.*, **76**, pp. 399–405.

[3] Krebs, H. I., Hogan, N., Aisen, M. L., and Volpe, B. T., 1998. "Robot-aided neurorehabilitation". *IEEE Transactions on Rehabilitation Engineering*, **6:1**, pp. 75–87.

[4] Mehrholz, J., Werner, C., Kugler, J., and Pohl, M., 2007. "Electromechanical-assisted training for walking after stroke (review)". *The Cochrane Collaboration*, **4**.

[5] Behrman, A. L., and Harkema, S. J., 2000. "Locomotor training after human spinal cord injury: A series of case studies". *Phys. Ther.*, **80(7)**, pp. 688–700.

[6] Hesse, S., Bertelt, C., Jahnke, M. T., Schaffrin, A., Baake, P., Malezic, M., and Mauritz, K. H., 1995. "Treadmill training with partial body weight support compared with physiotherapy in nonambulatory hemiparetic patients.". *Stroke*, **26(6)**, pp. 976–981.

[7] Hidler, J., Nichols, D., Pelliccio, M., Brady, K., Campbell, D. D., Kahn, J. H., and Hornby, T. G., 2009. "Multicenter randomized clinical trial evaluating the effectiveness of the lokomat in subacute stroke". *Neurorehabilitation and Neural Repair*, **23**, pp. 5–13.

[8] Roy, A., Krebs, H. I., Williams, D., Bever, C. T., Forrester, L. W., Macko, R. M., and Hogan, N., 2009. "Robot-aided neurorehabilitation: A robot for ankle rehabilitation". *IEEE Transaction on Robotics*, **25:3**, pp. 569–582.

[9] Peshkin, M., Brown, D. A., Santos-Munn, J. J., Makhlin, A., Lewis, E., Colgate, J. E., Patton, J., and Schwandt, D., 2005. "KineAssist: A robotic overground gait and balance training device". *Proceedings of the IEEE 9th International Conference on Rehabilitation Robotics*, pp. 241–246.

[10] Reinkensmeyer, D. J., Aoyagi, D., Emken, J. L., Galvez, J. A., Ichinose, W., Kerdanyan, G., Maneekobkunwong, S., Minakata, K., Nessler, J. A., Weber, R., Roy, R. R., de Leon, R., Bobrow, J. E., Harkema, S. J., and Edgerton, V. R., 2006. "Tools for understanding and optimizing robotic gait training". *Journal of Rehabilitation Research & Development*, **43:5**, pp. 657–670.

[11] Veneman, J. F., Kruidhof, R., Hekman, E. E. G., Ekkelenkamp, R., Asseldonk, E. H. F. V., and van der Kooij, H., 2007. "Design and evaluation of the lopes exoskeleton robot for interactive gait rehabilitation". *IEEE Transactions on Neural Systems and Rehabilitation Engineering*, **15:3**, pp. 379–386.

[12] Pohl, M., Werner, C., Holzgraefe, M., Kroczek, G., Mehrholz, J., Wingendorf, I., Hoolig, G., Koch, R., and Hesse, S., 2007. "Repetitive locomotor training and physiotherapy improve walking and basic activities of daily living after stroke: a single-blind, randomized multicentre trial (Deutsche Gang trainer Studie, DEGAS)". *Clinical Rehabilitation*, **21**, pp. 17–27.

[13] Jezernik, S., Colombo, G., and Keller, T., 2003. "Robotic orthosis Lokomat: a rehabilitation and research tool". *Neuromodulation*, **6**, pp. 108–115.

[14] Mayr, A., Kofler, M., Quirbach, E., Matzak, H., Frhlich, K., and Saltuari, L., 2007. "Prospective, blinded, randomized crossover study of gait rehabilitation in stroke patients using the lokomat gait orthosis". *Neurorehabilitation and Neural Repair*, **21**, pp. 307–314.

[15] Hornby, T. G., Campbell, D. D., Kahn, J. H., Demott, T., Moore, J. L., and Roth, H. R., 2008. "Enhanced gait-related improvements after therapist-versus robotic-assisted locomotor training in subjects with chronic stroke: a randomized control study". *Stroke*, **39**, pp. 1786–1792.

[16] Edgerton, V. R., Roy, R. R., de Leon, R. D., Tillakaratne, N., and Hodgson, J. A., 1997. "Does motor learning occur in the spinal cord?". *Neuroscientist*, **3**, pp. 287–294.

[17] Bosecker, C. J., and Krebs, H. I., 2009. "MIT-Skywalker". *Proc. of IEEE Int. Conf. on Rehabilitation Robotics*, pp. 542–549.

[18] Collins, S., Wisse, M., and Ruina, A., 2001. "A three-dimensional passive-dynamic walking robot with two legs and knees". *The International Journal of Robotics Research*, **20**, pp. 607–615.

[19] Murray, M. P., Drought, A. B., and Kory, R. C., 1964. "Walking patterns of normal men". *Journal of Bone & Joint Surgery*, **46A**, pp. 335–360.

[20] Artemiadis, P. K., and Krebs, H. I., 2010. "On the control of the mit-skywalker". *IEEE Engineering in Medicine and Biology Society, (under submission)*.

[21] Stauffer, Y., Allemand, Y., Bouri, M., Fournier, J., Clavel, R., Metrailler, P., Brodard, R., and Reynard, F., 2008. "Pelvic motion measurement during over ground walking, analysis and implementation on the walktrainer reeducation device". *Proc. of the IEEE/RSJ International Conference on Robots and Systems*, pp. 2362–2367.